CHAPTER FIFTEEN

A Quantitative Method for Measuring Phototoxicity of a Live Cell Imaging Microscope

Jean-Yves Tinevez,* Joe Dragavon,* Lamya Baba-Aissa,* Pascal Roux,* Emmanuelle Perret,* Astrid Canivet,* Vincent Galy,† *and* Spencer Shorte*

Contents

Abstract

Fluorescence-based imaging regimes require exposure of living samples under study to high intensities of focused incident illumination. An often underestimated, overlooked, or simply ignored fact in the design of any experimental imaging protocol is that exposure of the specimen to these excitation light sources must itself always be considered a potential source of phototoxicity. This can be problematic, not just in terms of cell viability, but much more worrisome in its more subtle manifestation where phototoxicity causes

* Institut Pasteur, Imagopole, Plateforme d'imagerie dynamique, Paris, France
† UMR7622, CNRS-UPMC, 9 quai St Bernard, Paris, France

Methods in Enzymology, Volume 506
ISSN 0076-6879, DOI: 10.1016/B978-0-12-391856-7.00039-1

anomalous behaviors that risk to be interpreted as significant, whereas they are mere artifacts. This is especially true in the case of microbial pathogenesis, where host–pathogen interactions can prove especially fragile to light exposure in a manner that can obscure the very processes we are trying to observe. For these reasons, it is important to be able to bring the parameter of phototoxicity into the equation that brings us to choose one fluorescent imaging modality, or setup, over another. Further, we need to be able to assess the risk that phototoxicity may occur during any specific imaging experiment. To achieve this, we describe here a methodological approach that allows meaningful measurement, and therefore relative comparison of phototoxicity, in most any variety of different imaging microscopes. In short, we propose a quantitative approach that uses microorganisms themselves to reveal the range over which any given fluorescent imaging microscope will yield valid results, providing a metrology of phototoxic damage, distinct from photobleaching, where a clear threshold for phototoxicity is identified. Our method is widely applicable and we show that it can be adapted to other paradigms, including mammalian cell models.

1. Introduction

In our experience, running the imaging facilities at the Institut Pasteur in Paris (www.imagopole.org) managing phototoxicity is critical to long-term live cell imaging studies on infectious processes. Host cell–pathogen interactions are especially challenging when it comes to their reconstitution within the context of meaningful experimental imaging paradigms, and phototoxic effects are an abundant source of problems. For example, approaches using multidimensional live cell imaging for studies on infection have become near routine as recourse to analyze subcellular dynamics (Frischknecht and shorte, 2009; Shorte and Frischknecht, 2008). The difficulty of such approaches comes from the need to maintain spatial and temporal resolution using protocols that assure over-sampling x, y, z, and t. To achieve this, automated, high-speed acquisition aims to sample x, y "stacks" as rapidly as possible to satisfy the requirement that 3D volumes are acquired in a snapshot. Further, the 3D stack must be repeatedly sampled over time at a frequency determined by the temporal dynamics of the process being recorded. Add to this the need for multiple wavelength channels acquired at any given moment, allowing to distinguish distinct targets, which must then be colocalized, it is not uncommon to require 50–150 images to be acquired at each time point. This can amount to the need for an elevated *light budget*. Overcoming the limitations imposed by this light budget can often be the key to successful imaging. In the context of a real study, for example, following fluorescently labeled HIV virus (Arhel *et al.*, 2006), bacteria (Enninga *et al.*, 2005), parasites (Amino *et al.*, 2006, 2007; Thiberge *et al.*, 2007), or prion protein (Gousset *et al.*, 2009), the need for extensive light exposure can have substantial impact

on the quality of the data, due to photobleaching that comprises the signal-to-noise ratio of the detectable signal, and phototoxicity that risks to perturb the processes under study.

A common misconception is to equate photobleaching with phototoxicity. Photobleaching is specific to fluorescence microscopy and arises due to the loss of fluorescent signal that occurs when fluorophores are excited into a state leading to an irreversible loss of signal. Phototoxicity, on the other hand, is a related phenomenon inasmuch as it may be precipitated by photobleaching of fluorophores, but not necessarily. It may also occur in the absence of fluorophore. Phototoxicity is a generalized term used as a catch-all to describe how exogenous light energy may interact with the tissue/cell metabolism (for detailed and extensive review, see Diaspro *et al.*, 2006). The term certainly refers to all those diverse processes resulting in light-induced free-radical generation, for example, from fluorescent labels, and/or light-sensitive metabolites. However, it also describes indirect effects such as localized thermal flux generation (undesired light-induced heating effects); light-induced ionizing, polarizing, and/or trapping effects; and of course unintended light-induced activation of membrane conductances. In turn, phototoxicity may result in extreme phenotypes such as cataclysmic cell death by, for example, free radicals rupturing cell membranes, and collapsing chemical and ionic compartmentalization. Such behaviors are easy to detect and reject before further analysis is performed. On the other hand, and much more problematic, phototoxicity may cause subtle effects, which are difficult to detect, or even distinguish because they do not kill the tissue, but rather subvert its functions. In the case of quantitative light microscopy, there is no ground truth inasmuch as it is the experimental device itself, the microscope, which induces these effects meaning that even careful control experiments may not be sufficient. Thus, our only remaining recourse to managing phototoxicity is to measure it and minimize risks by experimental design. Unfortunately, this is not a trivial task.

2. Measuring Phototoxicity

2.1. The need for a quantitative, generic, and convenient measure of phototoxicity

While it is rather well known, and somewhat implicit, that the impact of phototoxicity will vary with the amount of light delivered to the sample, much less clear are its underlying mechanisms. For example, while every biologist using live cell microscopy techniques will have an opinion on the subject, it is hard to know how a single-point-scanning confocal microscopy may be better or worse than, say, a multi-point-array-scanning confocal or a wide-field microscope. This uncertainty is due mainly to the

difficulty associated to quantifying phototoxicity; that is to associate a number relating the impact of phototoxicity of a specific imaging configuration, which can be used to compare different imaging configurations. Indeed, there are currently no systematic methods described in the literature enabling to directly measure and thereby quantifying phototoxicity.

In efforts to measure phototoxicity, many studies have side-stepped the difficult problem by exploiting the relative ease by which photobleaching can be measured as the time-dependent decay of fluorescent intensity coming from a known quantity of fluorophore. Such studies extrapolate their conclusions to be relevant to understanding phototoxicity in live biological targets reasoning implicitly the relationship between the two phenomena (De Vos *et al.*, 2009; Hoebe *et al.*, 2008). However, this is far from satisfactory because while phototoxicity and photobleaching processes may, in many instances, be tightly coupled, they are nonetheless distinctly separate phenomena. The literature does offer some examples of efforts to directly assess phototoxicity. For example, the group of Eric Manders monitored cell rounding (a secondary indicator of apoptosis; Bortner and Cidlowski, 2002) in the illuminated field of view providing evidence supporting the claim that their method of controlled light exposure microscopy diminished phototoxicity, by reducing total exposure to incident illumination (De Vos *et al.*, 2009; Hoebe *et al.*, 2008). In a more quantitative approach, similar methods counted the proportion of dead cells appearing during the few days following illumination by a mercury lamp in an epifluorescence microscope (Zdolsek *et al.*, 1990) or the number of cells able to form a colony after irradiation in epifluorescence (Wagner *et al.*, 2010) or multi-photon imaging (König *et al.*, 1999). Cell rounding, blebbing, and/or nuclear fragmentation were taken as indicative of cell death, but no data on incident light dose were reported. Studying tobacco cells, Dixit and Cyr (2003) went further toward a metrology of phototoxicity, monitoring cell death a few days after illumination, as a function of the measured incident light dose. While all these examples use phenotypic manifestation of cell death as a measure of phototoxicity, it is rather the worst case scenario that phototoxicity may cause much more subtle effects. For instance, Nishigaki *et al.* (2006) noticed that at high incident light, the beating of the flagella of human sperm is detectably slowed, although they did not quantify the effect. During intravital imaging in living Syrian golden hamsters, Saetzler *et al.*, 1997 report that a high incident light dose can induce uncontrolled leukocyte activation and adhesion in venules and arterioles, a crucial point when studying inflammatory response. The number of activated leukocytes was measured for a given period of time and analyzed as a function of the incident light dose. In neuron calcium imaging, it was observed that the dynamic range of Ca^{2+} pulses was impaired by a strong illumination power (Ji *et al.*, 2008; Koester *et al.*, 1999).

From these previous studies, it is clear that the challenge in measuring phototoxicity is its multifarious and non-continuous nature, which is

intractably linked to the particularity and specificity of the biological system under study. Indeed, phototoxicity may only ever be rather arbitrarily measured by following specific parameters in a given biological model. In this case, such parameters must be recorded in a defined experimental paradigm and should be sensitive enough to detect early effects, far upstream from cell death, but far enough downstream from the multiplicity of complex *de novo* light-induced processes so as to be robust, and reproducible over a relevant range of light dose. Toward this goal, we describe herein the rationale and method, proposing a protocol that yields a well-defined number that can be used as a quantitative measure of the tendency of an imaging system to evoke phototoxicity. We validate our approach by showing that this number is a characteristic of the illumination modality of the setup and can be used to compare different settings on the same setup, and even different setups.

2.2. A protocol to quantify the phototoxic effect of a microscopy system

In this study, we aimed to establish a method allowing phototoxicity to be compared between different imaging systems. The criteria for optimization of this method were as follows:

- *Quantitative*. The method should provide a simple readout for phototoxicity and a means to measure the relative power of light illuminating the living specimen therein. Quantification of these parameters must be reproducible and have a limited error range.
- *Generic*. Measurements must be easy to achieve and transpose readily between different imaging configurations and different imaging systems, ideally allowing to compare different illumination modalities based upon their phototoxic impact.
- *Convenient*. The method must be easily disseminated and implemented; it must be highly reproducible, lending itself ideally to become a standard amenable to be shared among different laboratories, and stable over time.

2.2.1. Experimental rationale

Caenorhabditis elegans is a free-living, transparent nematode (roundworm), about 1 mm in length, which lives in temperate soil environments. The molecular and developmental biology of *C. elegans* is well documented since over 30 years (Sulston and Horvitz, 1977). As a multicellular eukaryote, *C. elegans* is a valuable model organism offering distinct advantages. On a practical level, it is simple enough to be studied in great detail. Strains are cheap to breed and are fully viable after reanimation following long-term frozen storage. Further, from embryo to mature worm, *C. elegans* is transparent to visible light, facilitating the study of cellular differentiation and

other developmental processes. Imaging techniques can be applied in the intact organism, and by consequence, the developmental fate of every single somatic cell (959 in the adult hermaphrodite; 1031 in the adult male) has been mapped out (Kimble and Hirsh, 1979; Sulston and Horvitz, 1977).

These patterns of cell lineage are largely invariant between individuals, and recent live cell studies have revealed the dynamics of cell lineage in living embryos during the first 3 h of embryogenesis (Bao *et al.*, 2008). Bao *et al.* measured the cell cycle length from the one cell stage up to seven cycles of division for 20 embryos. Remarkably, the "developmental clock" variability showed the bifurcation of the lineage tree (the timing of nuclear division events) occurred with a remarkably small standard deviation ($< 4.5\%$). Presumably, this variation is due to the small variation of experimental conditions such as temperature; and the r^2 ranging 0.997–0.999 asserts that, on average, 95% of the cell divisions in the *C. elegans* embryo deviate less than 2% from the general clock. So, during embryogenesis, the *C. elegans* cell fate is tightly controlled and highly reproducible from one embryo to another.

While such studies validate the use of epifluorescence microscopy to monitor apparently healthy embryogenesis, at least during some period of time, *C. elegans* embryogenesis is actually exquisitely sensitive to epifluorescent illumination. In our own studies, we have found that increased incident illumination can result in disruption of cell division over time, specifically causing a retardation of the developmental clock. Further, this effect is easily detected by a reduction in the number of cell nuclei expected to be present at any given time during the lineage. Reasoning that the light sensitivity of *C. elegans* embryogenesis might be considered a phototoxicity paradigm, we tested whether this parameter (number of cell nuclei) was sensitive to light exposure in a dose-dependent, predictable, and reproducible manner.

2.2.2. Protocol content

2.2.2.1. Establishing imaging parameters We aimed to establish an experimental protocol to test the hypothesis that phototoxicity effects on *C. elegans* embryogenesis might manifest as a quantifiable relationship between the number of cell divisions and incident light exposure. Thus, the ideal protocol would reveal changes in the number of *C. elegans* cell divisions during early embryogenesis, attributable solely to variations in the incident light dose. Inasmuch as we hoped to use the method to compare the performance of a broad range of different imaging microscope systems, and configurations, relevant to real multidimensional imaging applications used in common experimental conditions, we designed a protocol exploiting the inherent flexibility and generic nature of a multidimensional time-lapse (Fig. 15.1). The light exposure cycle was repeated during the first 2 h of embryogenesis, starting from the onset of the first anaphase. The advantage of this approach was that it is relevant to real experimental conditions common to most live imaging experiments, and it ensured that the whole embryo

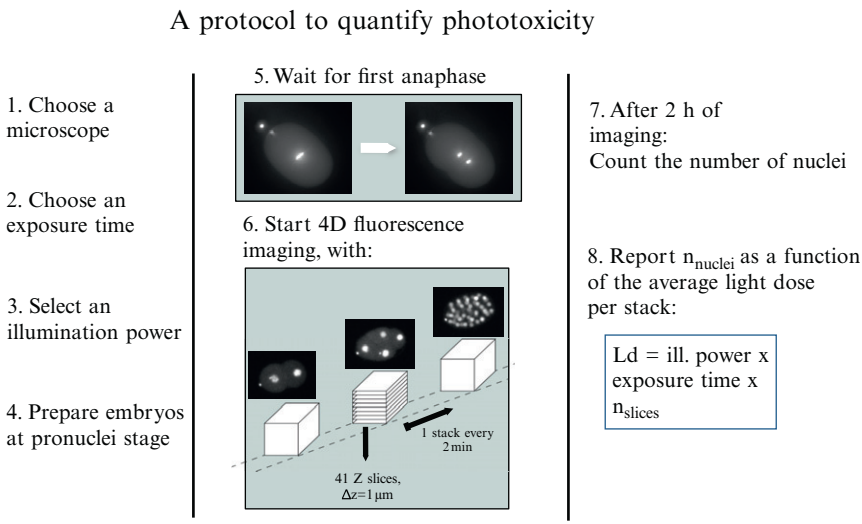

Figure 15.1 Summary of the protocol for the quantification of phototoxicity impact.

volume was subjected to comparable levels of light, rather than say, for example, a finite, focused, high-intensity light exposure like that used in FRAP experiments. Further, the protocol is relevant to those used for experimental imaging of *C. elegans* embryo elsewhere (Bao *et al.*, 2008, 2006).

2.2.2.2. Incident light dose measurements To compare *C. elegans*-based phototoxicity measurements on different imaging systems, or using different system configurations, it was necessary to find a means to quantify incident light delivered during the optimized acquisition protocol by measuring the light dose at the sample level. While it sounds simple, this is actually a non-trivial task. In developing the protocol presented here, we chose to report this quantity as the energy density dose deposited on the sample, when acquiring one stack, calculated as follows:

For epifluorescence wide-field microscopes and spinning-disks

- Measure the time-averaged power density at the sample level using the power set for imaging;
- Derive the light dose by multiplying the measured power by the exposure time per image, times the number of image acquisition in one stack (41 in our case).

This assumes that the whole embryo received 41 times the light energy used to image one place. Indeed, for these two systems, the whole fluorescent volume is excited, even if in the spinning-disk case, pinholes allow to collect light emitted from a single plane only.

2.2.2.3. Preparation of a selected C. elegans *strain for imaging* We chose the *C. elegans* strain AZ212 (Praitis *et al.*, 2001), which expresses the nuclear localized histone protein H2B, conjugated with eGFP (heterogeneous expression). Worms plated on Petri dishes containing agar-based growth support, supplemented for nourishment by inoculation with *Escherichia coli* bacteria, were maintained in a temperature-controlled bench incubator at 20 °C. Worm culture dishes were replated, depending on the experimental needs, every 1–4 days. H2B-GFP *C. elegans* embryos were prepared as described elsewhere (Bao *et al.*, 2008, 2006). Briefly, two to three hermaphrodite adult worms were plated on a coverslip in a droplet of M9 medium. Using a binocular stereomicroscope, the adult worms were dissected, and the eggs are dispersed. The egg-bearing coverslip was pressed onto a glass slide coated with agar 2% and sealed using valap. The sample slide set on a microscope system allowed eggs at the zygote stage to be selected for imaging.

2.2.2.4. C. elegans *imaging and phototoxicity impact quantitation* *C. elegans* embryogenesis was followed during 2 h from the first metaphase after pronuclei fusion, a non-ambiguous event in embryo development. From this precise moment, the developing embryo was subjected to an optimized light exposure protocol using an epifluorescent microscope system (ambient temperature range 20–22 °C). Conveniently, for the H2B-GFP strain used here, the first anaphase manifests as the first instant where two dense chromatin fluorescent spots can be seen and clearly separated. Two minutes before, when the fusion of the two pronuclei is complete, the cell is in metaphase and only one bright spot can be seen. The transition from metaphase to anaphase (Fig. 15.2) defines clearly an instantaneous temporal start point in the *C. elegans* embryo development from which subsequent cell division times may be measured. The occurrence of this event can be monitored with moderate fluorescent light, and it is also possible for the trained eye to see it with transmitted light.

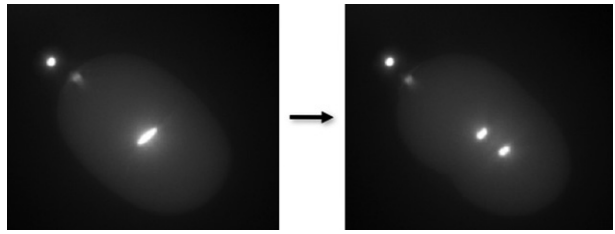

Figure 15.2 Left: *C. elegans* H2B-GFP embryo in metaphase. Chromatin appears as a single, compact, dense spot. Right: The same embryo in anaphase (2 min after Fig. 15.1). Two dense spots can now be seen. This event is used to determine precisely the onset of imaging. Images were acquired on a Zeiss wide-field epifluorescence inverted microscope, using a 63×-oil immersion objective.

Using the optimized protocol, individual embryos were exposed to repeated cycles of excitation light exposure on the imaging system in a multidimensional (x, y, z, t) acquisition protocol that was strictly fixed for all subsequent embryos. This way, a regular frequency of light exposure starting from the onset of the first anaphase was maintained until 2 h after this event (equivalent to seven cell division cycles in the non-phototoxic case). Thus, the whole embryo volume was exposed to excitation light by virtue of a z-stack acquisition, 41 z-axis "slices" (spaced by 1 μm) collected as rapidly as possible, once every 2 min during the 2 h. Depending on the imaging system, the frame exposure time was chosen according to an expected optimal range, and then fixed throughout, and for all subsequent embryos. Inasmuch as the image-data *per se* were not used in any subsequent analysis, it did not matter what image quality resulted from under-, or over-exposure of the detector. On the other hand, while the rhythm and frequency of light delivery was fixed for all embryos in any given analysis, the total light exposure was graded by varying the incident power at the light source. At the end of each run, the total number (N) of cells distributed throughout the embryo volume was counted (Fig. 15.3).

2.2.3. Impact of phototoxicity on *C. elegans* embryogenesis

Under conditions where no phototoxicity occurred, and at 20–22 °C, the total number of nuclei after 2 h is expected to be 46–54. Many embryos were imaged using exactly the same experimental conditions, and acquisition protocol, but gradually increased incident illumination resulted in data that could be represented as the number of nuclei versus light dose. Thus, without changes in the rate of light exposure, a clear effect of increased

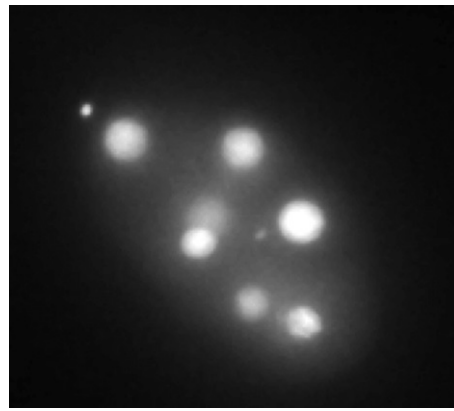

Figure 15.3 The same embryo that of Fig. 15.2, 2 h after the onset of anaphase. For the very high incident light dose used for imaging, the measured number of cells at this stage was only seven.

excitation light intensity was to diminish the number of cells, consistent with the expected adverse effect of excitation light exposure on cell division (Fig. 15.4). Indeed, the pattern of data from many embryos revealed that low levels of incident excitation illumination caused little phototoxicity, but at a threshold caused a sharp decline in the number of nuclei, above which this diminution increased in a manner proportional to increased light power, until embryogenesis was completely and cataclysmically arrested (Fig. 15.4). This sigmoidal relationship between the number of nuclei and incident light power was reproducible, and predictable, entirely consistent with our expectations, that the decrease is attributable to photodamage, quantifiable with respect to the incident light dose. On this curve, a single point represents the imaging of a *C. elegans* embryo for at least 2 h. Finally, to study the effect of increasing light dose, it was necessary to increase incident light dose over a broad range of relevant intensities using multiple embryos for each experimental run. The data pooled from at least 10 embryos allowed a conclusion on the threshold of light dose wherein the given microscopy system retarded embryogenesis, the point of inflexion being deemed as the "phototoxicity threshold." More precisely, the data are fit by a sigmoid, the simplest curve reflecting the observed distribution of points in the phototoxicity curve. From this fit, one can then derive the location of the inflexion point, with a 95% confidence interval, which we define as the phototoxicity threshold of a system under some specific imaging conditions (Fig. 15.4).

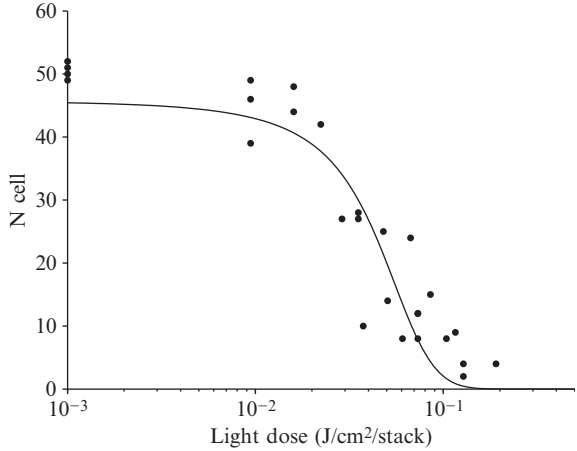

Figure 15.4 An example of a phototoxicity curve measured on a wide-field microscope. Dots are individual measurements; straight line is a fit by a sigmoid. The fit yields a phototoxicity threshold of 4.27×10^{-2} J/cm^2/stack (95% confidence interval is 3.65×10^{-2} to 4.88×10^{-2} J/cm^2/stack).

Parenthetically, data point variance may have arisen due to the difficulty to avoid small ambient temperature variations, as suggested in another study (Bao *et al.*, 2008). In the current studies, our environmental control was sufficient to limit a temperature range within a few degrees (21 ± 1 °C). On this point, it is important to stipulate the importance of environmental temperature. In separate studies, we found that at temperatures below 18 °C, *C. elegans* embryogenesis is significantly retarded. For example, at 17–18 °C and without illuminating the sample, we found that $N = 21–25$, compared to a range of 46–54 expected with a temperature of 20–22 °C. On the other hand, embryogenesis was accelerated such that $N = 60–72$ at temperatures in the range 23–25 °C, whereas above this range, embryogenesis lasted only a few cell divisions.

2.2.4. Understanding the meaning of phototoxicity curves

The shape of the phototoxicity threshold curves was predictable inasmuch as it could be understood as the accumulation of three distinct phases according to different light dose ranges (see Fig. 15.4):

2.2.4.1. Neutral phototoxicity at low-energy light dose The number of cells measured 2 h after imaging does not depend on the incident light leading us to the conclusion that in this dynamic context, no phototoxicity occurs. That is to say that if there is any phototoxicity occurring we do not detect it, either because our method is not sufficiently sensitive or the intrinsic dynamic mechanisms of the embryo (e.g., cytoplasmic mechanisms for free-radical management) are sufficient to minimize phototoxicity. It is noteworthy that the worm is a terrestrial animal that lives in soil and feeds on the bacteria growing on vegetative detritus, as such it may be equipped with some capacity to protect itself from occasional exposure to potentially hazardous ultraviolet sunlight, but presumably with only limited capacity able to deal with acute, and not chronic, exposure. In any case, at low light doses, the measured number of cells is the same whether we illuminate the sample or not. Consequently, this part of the curve is a plateau at $N = 46–54$ cells. The existence of an energy range where there is no visible phototoxic effect was observed in other studies (De Vos *et al.*, 2009; Dixit and Cyr, 2003).

2.2.4.2. Cumulative phototoxicity at intermediate range Above a certain light dose level, the timing of embryogenesis is impaired, observed as a temporal retardation in embryogenesis. Consequently, the number of cells measured 2 h after the onset of anaphase decays with increasing light dose. The fact that moderate incident light dose above a certain threshold can generate a dose-dependent phototoxic damage is consistent with previous studies showing single cell induced-phototoxic effects (Ji *et al.*, 2008; Koester *et al.*, 1999; Nishigaki *et al.*, 2006) and other studies in cell populations (Dixit and Cyr, 2003; König *et al.*, 1999; Saetzler *et al.*, 1997; Wagner *et al.*, 2010;

Zdolsek *et al.*, 1990). We also report that in this range of energy, the more incident light, the more damage is accrued in an apparently linear manner as evidence by the characteristic decay of the phototoxicity curve.

2.2.4.3. Cataclysmic phototoxicity at high-energy light dose For very high incident energy, severe damage is predicted, resulting in a total and complete arrest of embryo development, as soon as after the first or second cell division. Consequently, the phototoxicity curve goes through a point of inflexion, leading to a nadir at $N = 2$–4 cells. In this range of energy, our protocol cannot distinguish between different amounts of damage, for it reports only a constant number of cells. However, given that all relevant, physiological dynamic function is lost, the value of further analysis for the purpose of achieving optimum conditions for dynamic cellular imaging is obviated. At this stage, we are restricted to study the processes of photon-induced pathophysiology.

2.3. Longer image exposure times are less phototoxic

To further validate the developed method and to test its sensitivity, we next used it to measure phototoxicity under conditions where changes in the image acquisition regime should give predictable effects. We compared exactly the same image acquisition protocol except the camera exposure time used to acquire each image in each stack was increased from 100 to 500 ms. The effect upon phototoxicity curves, given the same total light dose, demonstrates that the latter would be less phototoxic due to the lower rate of light delivery (Fig. 15.5). Indeed, the shift of the phototoxicity curve to the right indicates that the phototoxicity threshold is higher under the image acquisition regime using longer exposure times. That is to say empirically that our method revealed that delivery of the same total amount of light energy, except more slowly, is less phototoxic than delivery of the same total light energy in less time. This observation is consistent with the expectation that the *rate* and *intensity* of light delivery are important factors in increasing risk of phototoxic damage to live cells (Amino *et al.*, 2007).

2.4. Using phototoxicity curves to compare microscope-based imaging systems

Given some constraints, an exciting perspective of our method for measuring phototoxicity is that it offers an easily distributed, common standard (H2B-GFP *C. elegans*) and protocol allowing direct comparison of different microscope systems anywhere. Indeed, precisely reproducing the protocol generates standard phototoxicity curves based on definite variables, which are independent from intensity-based image analysis or image quality. The curves using these well-defined, robust variables (total light dose energy

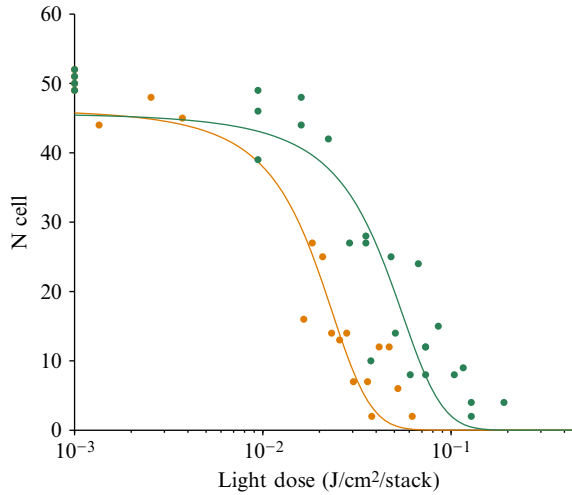

Figure 15.5 Two phototoxicity curves, acquired on the same wide-field system, differing only in the exposure time per slice. Orange: exposure time is 100 ms. Green: 500 ms. The phototoxicity thresholds are, respectively, 1.85×10^{-2} [1.57×10^{-2} to 2.13×10^{-2}] and 4.27×10^{-2} [3.65×10^{-2} to 4.88×10^{-2} J/cm^2/stack (value and (95% confidence interval)].

versus the number of nuclei) can therefore be compared, no matter their original source or time, and may be used to compare microscopy systems, by simple curve overlay.

Using this approach, Fig. 15.6 compares phototoxicity on two setups so far:

- A spinning-disk (an Andor Revolution system mounted on an inverted Zeiss AxioVert 200M and based on a CSU10 head) and
- A wide-field epifluorescence inverted microscope.

Total light energy doses reported use of measurements made from behind the objective and are not corrected for transmittance. Further, because we used objectives from the same series, comparative results hold valid. Comparatively, the two systems gave phototoxicity curves consistent with the expected characteristic properties. Namely, while some point dispersion inherent to biological noise was observed both phototoxicity curves resembled the characteristic shape predicted. In particular, a range of light dose with no measurable phototoxic effect was observed, and as the light dose was increased, this was accompanied by a dose-dependent phototoxicity effect culminating with developmental arrest. Our results demonstrate *a priori* that the spinning-disk illumination has a stronger phototoxic impact than plain wide-field illumination, yielding a phototoxicity threshold

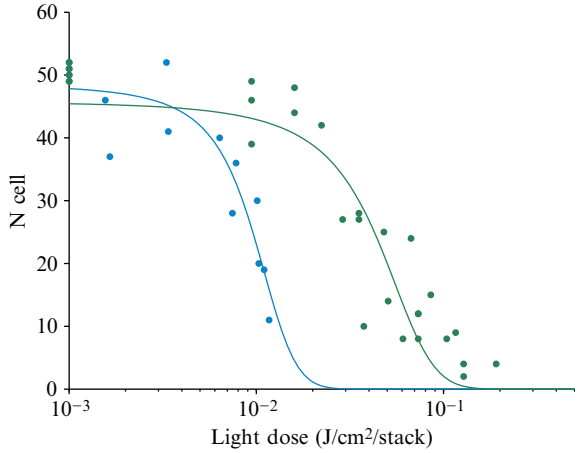

Figure 15.6 Two phototoxicity curves for two different systems using the same objective. Blue: a spinning-disk microscope using a Yokagawa CSU10 head. Green: a wide-field microscope. The phototoxicity thresholds are, respectively, 9.58×10^{-3} [8.58×10^{-3} to 1.06×10^{-2}] and 4.27×10^{-2} [3.65×10^{-2} to 4.88×10^{-2}] J/cm^2/stack.

of approximately 1×10^{-2} J/cm^2/stack for the spinning-disk, versus 4×10^{-2} J/cm^2/stack for the wide-field microscope.

3. Discussion

3.1. A live specimen-based metrology

In Life Sciences, microscopes are mainly used to gather information on live specimen. It is not surprising then that assessing the performance of these microscopes involve using a live sample, particularly when it comes to quantifying the impact of imaging on live specimen. Measuring other performance criteria may not require stepping in the complexity of dealing with live samples. The rate of photobleaching, for instance, focuses on a fluorophore and its environment. To measure it, one can very conveniently purchase commercially available probes coupled to latex beads that are easy to mount and can be stored reliably over an extended period of time without sample deterioration. Phototoxicity, on the other hand, is an effect observed on a living sample, and as such can only be quantified by taking a measurement on some dynamic property of this sample. Two key points are linked to this simple observation.

First, a proper live sample must be defined as a standard for measurements. Contrary to common imaging situations, these metrology experiments are

performed to get insight on the performance of microscopy systems, not on the live specimen, which can therefore be selected on the basis of convenience. Second, a measurable dynamic feature able to relate the impact of phototoxicity must be sought. Its baseline (its value when there are no phototoxic effects on the sample) must be known or measurable. Ideally, its numerical value is a robust, deterministic function of the incident light dose for a given system, safe from typical biological variations, so that the same measure taken several times with the same input gives a distribution with a very small deviation.

Various authors have proposed different models to quantify phototoxicity. Several studies are conducted based on monitoring the survival of cultured cells after a given light dose exposure (Dixit and Cyr, 2003; König *et al.*, 1999; Wagner *et al.*, 2010; Zdolsek *et al.*, 1990). Individual cell viability is assessed by a live-dead viability kit or direct observation of the cell's morphology. Saetzler *et al.* (1997) monitor leukocyte rolling and adhesion in arterioles and venules as a function of incident light dose during intravital imaging of golden hamsters. Two groups follow the dynamics of Ca^{2+} pulses, followed by fluorescence, elicited in rodent brain neurons as a measure of phototoxicity (Ji *et al.*, 2008; Koester *et al.*, 1999). All these methods give adequate and meaningful results, but are not trivial to disseminate. Maintaining any culture cell line, not mentioning living animals, requires equipment, people training, and administrative authorizations that can be a strain for a non-dedicated lab. Yet, a living sample-based metrology tool affordable by laboratories specialized in the development of imaging devices or industrial manufacturers would be beneficial to the imaging domain.

In this view, we choose to build our phototoxicity protocol using *C. elegans* embryo. The specific strain used here can be ordered from The Caenorhabditis elegans Genetics Center. The manipulation and mounting for imaging require only a basic stereomicroscope. Finally, their care and maintenance require very little expertise and equipment. Prior to this study, our lab had no expertise in or dedicated equipment for *C. elegans*. We sent some protocol kits to two remote labs, with no prior experience as well, and had them carry successful measurements on their systems. This demonstrates the portability of the protocol.

We chose to report the number of cells counted after 2 h of imaging for several reasons. We want to make a statement on the imaging effects that occur for long-term time-lapse 3D experiments, for which subtle artifacts can occur over a long period of time. We then must follow the embryogenesis over a time long enough to be meaningful for these experiments. Counting the number of cells is trivial in our case; in the strain we chose the nuclei are labeled with eGFP, we can simply use the last time point in the acquisition to make the measurement. Also, the number of cells 2 h post first anaphase is always tractable (50 for the baseline), yet it is large enough to allow for detectable drops when phototoxicity kicks in.

Another dynamic feature could have been chosen; for instance, measuring the time it takes for the embryo to reach the 28-cell stage. A strong phototoxicity effect would then manifest itself from having a much longer time to reach this stage. We chose, however, to count the number of cells after a given time, because it enables the extended use of this protocol:

- First, it can be used on non-imaging devices or on imaging devices for which a proper *C. elegans* embryo image cannot be formed (e.g., at low magnification or without detector). Since the delivery of the light (input) and the counting of the cells (measure) are decoupled, the embryo can be placed onto the device to be tested for the 2 h, then brought onto another suitable imaging device to count the number of cells.
- Second, it is not limited to measure damage caused by light. An embryo can be placed in a hostile environment (chemicals, radiations, etc.) for 2 h, then again brought to an imaging device to count cells.

3.2. The delivery rate of light dose matters for phototoxicity

We present a standard (H2B-GFP *C. elegans*) and method to measure directly the relationship between light intensity and phototoxicity on any imaging microscope system, configured to acquire data in any given optimized image acquisition regime. This allows us to estimate the "photon-light budget" available to any given experimental regime. Demonstrating its broad utility, we show the method applied to two relatively simple experimental paradigms: (i) changing image exposure times and (ii) changing the imaging system. In the first example, we clearly distinguished the phototoxicity cost that accompanies the need to use shorter exposure times with increased excitation intensities. This exigency is often stipulated by the need, for example, to image fast cellular events. Interestingly, our results suggest that the *rate* at which photons are delivered is critical to their eventual phototoxic impact. Along these same lines, a second series of experiments revealed spinning-disk microscopy to be more phototoxic than conventional wide-field epifluorescence illumination.

In their study on tobacco cells, Dixit and Cyr (2003) observed that for the same incident dose, the photodamage was more pronounced for a higher rate of illumination. That is, illuminating the sample with shorter exposures but higher power generates more photodamage than the converse. With the spinning-disk confocal illumination, we are in a situation where a point at the sample level receives light energy by short intense bursts. The pixel dwell-times for spinning-disk confocal are on the order of microseconds. This is to be compared with the 500 ms continuous illumination in the epifluorescence case. This rate-dependence might be due to the presence of "phototoxicity buffers" in the cell. The predominant process for phototoxicity generated by fluorescent imaging is thought to be a type II reaction (Zdolsek, 1993) where

reactive oxygen species (ROS) are generated by the energy transfer of an excited fluorophore in a triplet state to a molecule of oxygen, exciting it to a singlet state. The singlet oxygen can interact with other molecules within the cell and generate phototoxicity effects (Saetzler *et al.*, 1997). Natural ROS scavengers, such as glutathione, ascorbate, and tocopherol, allow the cell to cope with a certain amount of photodamage with no impact (De Vos *et al.*, 2009; Dixit and Cyr, 2003). If we suppose now that these scavengers have a regeneration rate with a timescale similar that of the photon illumination rate, then superior rates of photon delivery may overcome the protective metabolism leading to irreversible, cumulative photodamage. For a given incident light dose, a slower photon delivery rate, for example, imaging at longer exposure times with lower illumination power will be protective, allowing free-radical scavenger mechanisms to regenerate and cope with ROS. We assume in either regime the same amount of ROS is generated, but the lower illumination rate is permissive to metabolic management by ROS scavengers. We speculate that this is the reason why spinning-disk confocal compares unfavorably in this study. Our conclusion that increased illumination rate explains why spinning-disk confocal reported a decreased phototoxicity threshold (i.e., was more phototoxic) compared to wide-field is entirely consistent with our wide-field microscope data showing shorter (100 ms) exposure times are more phototoxic than long (500 ms) exposure times.

3.3. Comparing illumination modalities

It is often stated that spinning-disks are the optimal system when it comes to photobleaching (Vermot *et al.*, 2008), ergo photodamage, a conclusion challenged by the results presented here. However, it must be noted that this optimality statement is based on the fact that these systems are equipped with very sensitive cameras, and offer optical sectioning, that enable the use of a much lower light dose to reach an acceptable SNR (Inoue and Inoue, 2002). These two options are seldom used on conventional wide-field microscopes, and an experimenter trying to optimize the image quality instead of the incident light dose will likely find a spinning-disk to be optimal.

Because it involves solely the light dose measured at the sample level, our protocol characterizes the impact of the illumination path and delivery modality only. It does not take into account the image quality that depends on the detection path. This is a desirable feature for a metrology tool: it allows the investigation and optimization of one part of the system independently of the repercussion of other parts. However, practical cases of imaging strive at obtaining the best image quality under the constraint of minimal photodamage. The method proposed here does not take image quality into account, and we aim to reconcile these two aspects in a future work.

4. Conclusion

We present a method and standard providing a non-ambiguous and singular readout reporting the phototoxicity of any imaging microscope system. The method yields a phototoxicity threshold value, which can be used to compare configuration settings in the same modality or even other. The protocol was engineered to be portable and convenient, so that it can be used in any lab. Using this approach, we demonstrate spinning-disk confocal imaging to be characterized by a lower phototoxicity threshold (i.e., is more phototoxic) than a wide-field epifluorescence microscope, a result we interpret as due to the critical dependence of phototoxicity upon the rate of photon illumination. Consistent with this view, we show that in wide-field epifluorescence microscopy the same total light dose delivered by shorter exposure times is associated with higher phototoxicity (i.e., a lower phototoxicity threshold) than the same light dose delivered by longer exposure times.

ACKNOWLEDGMENTS

We thank Johan Henriksson for a stimulating discussion. This work was funded by the European Commission FP7 Health (project "LEISHDRUG", www.leishdrug.org, SLS) and ICT (project "MEMI", www.memi-fp7.org, SLS), the Conny-Maeva Foundation (USA), and the Institut Pasteur Paris. J.D. received a fellowship from the Pasteur-Foundation (New York).

REFERENCES

Amino, R., *et al.* (2006). Quantitative imaging of Plasmodium transmission from mosquito to mammal. *Nat. Med.* **12,** 220–224.

Amino, R., *et al.* (2007). Imaging malaria sporozoites in the dermis of the mammalian host. *Nat.Protoc.* **2,** 1705–1712.

Arhel, N., *et al.* (2006). Quantitative four-dimensional tracking of cytoplasmic and nuclear HIV-1 complexes. *Nat. Methods* **3,** 817–824.

Bao, Z., *et al.* (2006). Automated cell lineage tracing in Caenorhabditis elegans. *Proc. Natl. Acad. Sci. USA* **103**(8), 2707–2712.

Bao, Z., *et al.* (2008). Control of cell cycle timing during C. elegans embryogenesis. *Dev. Biol.* **318**(1), 65–72.

Bortner, C. D., and Cidlowski, J. A. (2002). Apoptotic volume decrease and the incredible shrinking cell. *Cell Death Differ.* **9**(12), 1307–1310.

De Vos, W. H., *et al.* (2009). Controlled light exposure microscopy reveals dynamic telomere microterritories throughout the cell cycle. *Cytometry A* **75**(5), 428–439.

Diaspro, A., *et al.* (2006). Photobleaching. *In* "Handbook of Biological Confocal Microscopy," (J. B. Pawley, ed.) 3rd edn, pp. 690–702.

Dixit, R., and Cyr, R. (2003). Cell damage and reactive oxygen species production induced by fluorescence microscopy: Effect on mitosis and guidelines for non-invasive fluorescence microscopy. *Plant J.* **36**(2), 280–290.
Enninga, J., *et al.* (2005). Secretion of type III effectors into host cells in real time. *Nat. Methods* **2**(12), 959–965.
Frischknecht, F., and Shorte, S. (eds.) (2009). Imaging host-pathogen interactions. *Biotechnol. J. (Special Edition)* **4**(6), 773–948, Wiley-Blackwell.
Gousset, K., *et al.* (2009). Prions hijack tunnelling nanotubes for intercellular spread. *Nat. Cell Biol.* **3,** 328–336.
Hoebe, R. A., *et al.* (2008). Quantitative determination of the reduction of phototoxicity and photobleaching by controlled light exposure microscopy. *J. Microsc.* **231**(1), 9–20.
Inoué, S., and Inoué, T. (2002). Direct-view high-speed confocal scanner: The CSU-10. *Methods Cell Biol.* **70,** 87–127.
Ji, N., *et al.* (2008). High-speed, low-photodamage nonlinear imaging using passive pulse splitters. *Nat. Methods* **5**(2), 197–202.
Kimble, N., and Hirsh, D. (1979). The postembryonic cell lineages of the hermaphrodite and male gonads in *Caenorhabditis elegans*. *Dev. Biol.* **70**(2), 396–417.
Koester, H. J., *et al.* (1999). Ca2+ fluorescence imaging with pico- and femtosecond two-photon excitation: Signal and photodamage. *Biophys. J.* **77**(4), 2226–2236.
König, K., *et al.* (1999). Pulse-length dependence of cellular response to intense near-infrared laser pulses in multiphoton microscopes. *Opt. Lett.* **24**(2), 113–115.
Nishigaki, T., *et al.* (2006). Stroboscopic illumination using light-emitting diodes reduces phototoxicity in fluorescence cell imaging. *Bio Techniques* **41**(2), 191–197.
Praitis, V., *et al.* (2001). Creation of low-copy integrated transgenic lines in *Caenorhabditis elegans*. *Genetics* **157**(3), 1217–1226.
Saetzler, R. K., *et al.* (1997). Intravital fluorescence microscopy: Impact of light-induced phototoxicity on adhesion of fluorescently labeled leukocytes. *J. Histochem. Cytochem.* **45** (4), 505–513.
Shorte, S., and Frischknecht, F (eds.) (2008). Imaging Cellular and Molecular Biological Functions, Springer-Verlag, Heidelberg, Germany.
Sulston, J. E., and Horvitz, H. R. (1977). Post-embryonic cell lineages of the nematode, Caenorhabditis elegans. *Dev. Biol.* **56**(1), 110–156.
The Caenorhabditis elegans Genetics Center page on AZ212 strain. https://cgcdb.msi.umn.edu/strain.php?id=5544.
Thiberge, S., *et al.* (2007). In vivo imaging of malaria parasites in the murine liver. *Nat. Protoc.* **2,** 1811–1818.
Vermot, J., *et al.* (2008). Fast fluorescence microscopy for imaging the dynamics of embryonic development. *HFSP J.* **2**(3), 143–155.
Wagner, M., *et al.* (2010). Light dose is a limiting factor to maintain cell viability in fluorescence microscopy and single molecule detection. *Int. J. Mol. Sci.* **11**(3), 956–966.
Zdolsek, J. M. (1993). Acridine orange-mediated photodamage to cultured cells. *APMIS* **101**(2), 127–132.
Zdolsek, J. M., *et al.* (1990). Photooxidative damage to lysosomes of cultured macrophages by acridine orange. *Photochem. Photobiol.* **51**(1), 67–76.